ESTIMATION OF HYDRODYNAMIC COEFFICIENTS OF A NONLINEAR MANOEUVRING MATHEMATICAL MODEL WITH FREE-RUNNING SHIP MODEL TESTS

(DOI No: 10.3940/rina.ijme.a3.2018.448)

Haitong Xu, M A Hinostroza and **C Guedes Soares** Centre for Marine Technology and Ocean Engineering (CENTEC), Instituto Superior Técnico, Universidade de Lisboa, Portugal

SUMMARY

Free-running model tests have been carried out based on a scaled chemical tanker ship model, having a guidance, control and navigation system developed and implemented in LabVIEW. In order to make the modelling more flexible and physically more realistic, a modified version of Abkowitz model was introduced. During the identification process, the model's structure is fixed and its parameters have been obtained using system identification. A global optimization algorithm has been used to search the optimum values and minimize the loss functions. In order to reduce the effect of noise in the variables, different loss functions considering the empirical errors and generalization performance have been defined and implemented in the system identification program. The hydrodynamic coefficients have been identified based on the manoeuvring test data of free-running ship model. Validations of the system identification algorithm were also carried out and the comparisons with experiments demonstrated the effectiveness of the proposed system identification method.

NOMENCLATURE

ρ	Density of water (kg m^{-3})
u	The forward velocity (m s^{-1})
v	The transverse velocity (m s^{-1})
u_c	The current's magnitude (m s^{-1})
α	The current's direction (rad)
ψ	The heading angle (rad)
u_r	The relative forward velocity (m s^{-1})
v_r	The relative transverse velocity (m s^{-1})
m	The mass of the ship (m)
$X_{\dot{u}_r}$	The added mass in x direction
$Y_{\dot{v}_r}$	The added mass in y direction
$Y_{\dot{r}}$	The added mass in r direction
$N_{\dot{v}_r}$	The added moment in y direction
$N_{\dot{r}}$	The added moment in r direction
c	The weighted average flow speed
A_P	The propeller area (m^2)
A_R	The rudder area (m^2)
ω	The wake fraction
$u_{A\infty}$	The induced axial velocity (m s^{-1})
K_T	The propulsive coefficient
D	The propeller diameter (m)
e	The effective rudder angle
$Coef_{new}$	The regression coefficient
κ_{Coef}	The adjustment coefficient
$Coef_0$	The hydrodynamic coefficients
d	The draft of the ship (m)
y_i	The target output
$\hat{y}_i$	The mathematical model output

1. INTRODUCTION

The accurate mathematical model for simulation of the manoeuvring motion of real vessels is of great importance. Some tools and methods have been developed to compute these mathematical models for simulation purposes. The determination of a reliable manoeuvring mathematical model for marine surface vehicles is still an important topic and demanding task (Eloot and Vantorre, 1998). The captive model tests are an effective method, which is widely used to obtain hydrodynamic coefficients of marine surface vehicles, but it is much expensive and time consuming. It also should be noted that hydrodynamics coefficients of manoeuvring motion can also be determined by other means, such as slender body theory, empirical formulae, computational fluid dynamics and system identification (Yoon and Rhee, 2003) In this sense, system identification is one of the highlights among the research topics in engineering and also play an important role in control of autonomous vehicles.

System identification (Ljung, 1987; Söderström and Stoica, 1989) has been widely used for mathematical modelling of dynamic systems (Söderström et al. 2003; Tang et al. 2014), robot simulation and training (Akanyeti et al. 2008; Iglesias el al. 2008; Kyriacou el al. 2008), and motion control (Åström and Källström, 1976; Tafner et al. 2014). The objective of system identification is to model the input-output behaviour of a system as well as possible. In (Schafroth et al. 2010), the parameters of a nonlinear dynamic model of a micro helicopter were identified using a nonlinear identification tool. A novel model identification methodology for ARX models based on transfer functions has been proposed by Kon et al.(2013).

The least square methods have been widely used for parameter estimation or white box modelling. For example, least-squares identification technology was used to estimate the parameters of nonlinear dynamic models in (Casenave et al. 2010). Alonge et al (2001) presented an offline GA-based identification method, which was used to estimate the parameters of motors. But the accuracy of least square methods is usually largely affected by the noise of training data and it usually leads to inconsistent estimates (Söderström, 2013). In order to solve the noise-corrupted in system identification, an errors-in-variable method has been proposed and plays an important role in mathematical modelling. In (Söderström, 2007; 2010), a general introduction on the background and motivation of errors-in-variables method was presented, and some example were also provided to demonstrate the effectiveness. In (Chen and Ljung, 2013), the regularized least-squares method was used to solve the hyper-parameter estimation problem with large data sets and ill-conditioned computations. Black box system identification is a purely data-driven modelling tool, which means that a priori structure of the system is not need.

Artificial Neural Networks (ANN) are one typical method for black box modelling and was used to model the manoeuvrability of a catamaran (Moreira and Guedes Soares, 2003, 2012). A radial basis function neural networks (NNs), which was employed to approximate the unknown ocean surface ship dynamics, is presented by Dai et al. (2012). Rajesh et al. (2010) investigated the performance of the neural network models for modelling nonlinear manoeuvring of ships. The advantage of ANN algorithm is that it does not imply any a priori structure of the ship mathematical model, but the disadvantage is that it cannot be extended, modified or tuned without full retraining which is not always possible (Sutulo and Guedes Soares, 2014, 2015).

The estimation of hydrodynamic coefficients of marine surface ships based on free-running model tests is always an interesting topic, which drew a great attention due to its effectiveness and accuracy (Luo et al. 2016; Sutulo and Guedes Soares, 2014, 2015; Yoon and Rhee, 2003; Zhang and Zou, 2011). Free-running model tests are often used to confirm manoeuvring properties of a ship configuration in the most direct and convincing way (Moreira and Guedes Soares, 2014; Perera et al., 2012).

In this paper, a scaled model of a chemical tanker has been built and one guidance, control and navigation platform also has been developed and implemented on the model. Various sensors (i.e. GPS, IMS and fibre-optic gyrocompass units) are integrated together in the LabVIEW platform. It consists of several program loops: FPGA loop, real-time loop and TCP/IP loop. The manoeuvring tests proposed by the Interim Standards for Ship Manoeuvrability (IMO) (ITTC, 2002) have been carried out in a swimming pool and the results are used for identify the parameters of the nonlinear manoeuvring mathematical model.

System identification for marine surface ship has always drawn a lot attention. Many researchers have been working on this topic. In (Åström and Källström, 1976), the parameters of a linear continuous time model were identified using the maximum likelihood method. Further work can be found in (Källström and Åström, 1981), where full-scale experiments have been used to demonstrate the effectiveness of system identification method for ship steering modelling. An extended Kalman filter (EKF) was applied to identify the parameters of a modified Nomoto model for vessel steering in (Perera, et al. 2016, 2015). System identification can also be used to obtain the parameters of a more complex manoeuvring model. For example, in (Revestido Herrero and Velasco González, 2012), a grey box approach has been used to identify of nonlinear manoeuvring model of marine vessels, a two-step approach was used to handle the modelling problem. A classical linear model was identified in the first step and a refinement has been carried out with the Kalman filter in the second step.

Recently the support vector machine, which was firstly used for classification, was applied to the regression purpose. Falck et al. (2012) presented an online least squares support vector regression for quality prediction. In (Luo et al., 2016; Luo et al. 2014; Zhang and Zou, 2011) support vector machine was used to identify manoeuvring model of Mariner class surface ship, but the validation carried out so far does not permit to draw definite conclusions about the effectiveness of this method (Sutulo and Guedes Soares, 2014). A modified version, Least Squares Support Vector Machines, was also used to identify the 2nd Nomoto model with real experimental data obtained from a zigzag manoeuvre made by a scaled ship (Luo et al., 2014; Moreno-Salinas et al., 2013). In (Xu and Guedes Soares, 2016a, 2016b), Least Squares Support Vector Machines was applied to model the controller of marine surface vehicle for path following scenarios.

In this paper, a nonlinear manoeuvring model was presented. To make the modelling more flexible and physically more realistic, modifications the Abkowitz model were introduced by including the rotation speed of the propeller and the flow velocity over the rudder. System identification is used to estimate the hydrodynamic parameters of an autonomous surface vehicle, whose *true* values of the hydrodynamic coefficients are not known before. Free-running model tests have been carried out based on a scaled chemical tanker ship model. Zigzag manoeuvring tests are used for identification purposes. Different metrics are defined considering the empirical errors and generalization performance, and a global optimization algorithm is implied to search the optimal parameters. At last, validation of the algorithm is carried out to verify the effectiveness of the proposed identification technology.

2. NONLINEAR MANOEUVRING MATHEMATICAL MODEL OF MARINE SURFACE SHIP

A ship in a seaway has 6 degrees of freedom (DOF) to move freely in the space, as illustrated in Figure 1. In order to simplify the problem of manoeuvring modelling, some assumptions need to be adopted. The heave, roll and pitch motion are not important in manoeuvring problem, as the ship moves in the horizontal plane. The coordinate frames of surface ship in 3 DOF are presented in Figure.2. In estimation theory, a mathematical model of surface marine ship is needed to describe the dynamics of the system. The Abkowitz (1980) model will be modified in order to make the modelling more flexible and realistic physically. In this study, the current effect is considered as the main external excitation, because the ship model has a small above water structure.

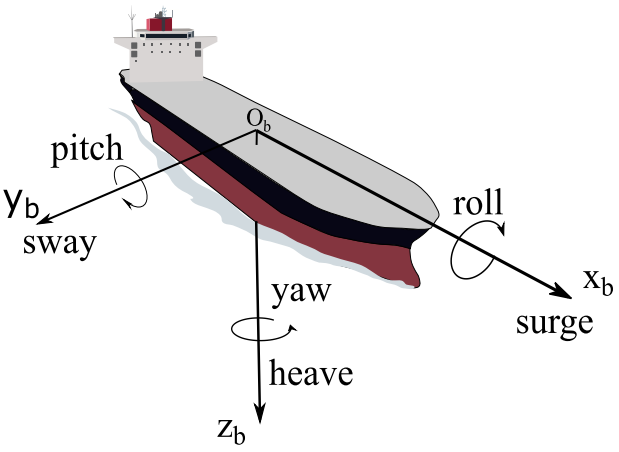

Figure 1: Motion of marine surface vehicle in 6 degree of freedom

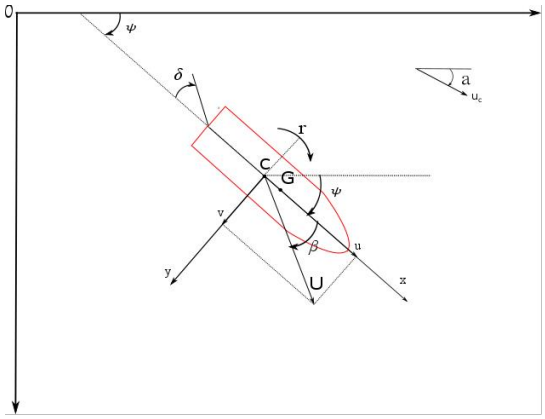

Figure 2: Coordinate frames for marine surface vehicle

As presented in figure 2, the relative forward velocity u_r and transverse velocity v_r are given by

$$\begin{aligned} u_r &= u - u_c\cos(\psi-\alpha) \\ v_r &= v + u_c\sin(\psi-\alpha) \end{aligned} \tag{1}$$

The time derivatives of u and v are given:

$$\begin{aligned} \dot{u} &= \dot{u}_r - u_c r\sin(\psi-\alpha) \\ \dot{v} &= \dot{v}_r - u_c r\cos(\psi-\alpha) \end{aligned} \tag{2}$$

where the accelerations of the motion in 3 degrees of freedom (surge, sway and yaw) are given in:

$$\begin{aligned} (m-X_{\dot{u}_r})\dot{u}_r - mv_r r - mx_G r^2 &= f_1 \\ (m-Y_{\dot{v}_r})\dot{v}_r + (mx_G - Y_{\dot{r}})\dot{r} + mu_r r &= f_2 \\ (m-N_{\dot{v}_r})\dot{v}_r + (I_z - N_{\dot{r}})\dot{r} + mx_G u_r r &= f_3 \end{aligned} \tag{3}$$

The dimensionless forces are defined as multi-variety third-order regression polynomials depending on the non-dimensional velocities. In equation (4), in order to model the ship in the surge, f_1 is divided into two parts. The thrust term and $f_1^{*\prime}$ is given by Eqs. (7-8)

$$f_1' = \kappa_{\eta_1}\eta_1' u_r'^2 + \kappa_{\eta_2}\eta_2' n' u_r' + \kappa_{\eta_3}\eta_3' n'^2 - \kappa_{C_R} C_R' + \kappa_{X_{v_r v_r}} X'_{v_r^2} v_r'^2 + \kappa_{X_{ee}} X'_{e^2} e^2 + \kappa_{X_{rr}} X'_{r^2} r'^2 + \kappa_{X_{v_r r}} X'_{v_r r} v_r' r' + \kappa_{v_r^2 r^2} X'_{v_r^2 r^2} v_r'^2 r'^2 \tag{4}$$

$$f_2' = \kappa_{Y_0} Y_0' + \left\{\kappa_{v_r} Y'_{v_r} v_r' + \kappa_{Y_\delta} Y'_\delta (c-c_0) v_r'\right\} + \left\{\kappa_{Y_r} Y'_r r' - \kappa_{Y_\delta} \frac{Y'_\delta}{2}(c-c_0) r'\right\} + \kappa_{Y_\delta} Y'_\delta \delta + \kappa_{Y_{rrv_r}} Y'_{r^2 v_r} r'^2 v_r' + \kappa_{Y_{eee}} Y'_{e^3} e^3 \tag{5}$$

$$f_3' = \kappa_{N_0} N_0' + \left\{\kappa_{N_{v_r}} N'_{v_r} v_r' - \kappa_{N_\delta} N'_\delta (c-c_0) v_r'\right\} + \left\{\kappa_{N_r} N'_r r' + \frac{1}{2}\kappa_{N_\delta} N'_\delta (c-c_0) r'\right\} + \kappa_{N_\delta} N'_\delta \delta + \kappa_{N_{rrv_r}} N'_{r^2 v_r} r'^2 v_r' + \kappa_{N_{eee}} N'_{e^3} e^3 \tag{6}$$

$$\text{Thrust } (u_r', n') = \kappa_{\eta_1}\eta_1' u_r'^2 + \kappa_{\eta_2}\eta_2' n' u_r' + \kappa_{\eta_3}\eta_3' n'^2 \tag{7}$$

$$f_1^{*\prime}(u_r', v_r', u', v', r', \delta) = -\kappa_{C_R} C_R' + \kappa_{X_{v_r v_r}} X'_{v_r^2} v_r'^2 + \kappa_{X_{ee}} X'_{e^2} e^2 + \kappa_{X_{rr}} X'_{r^2} r'^2 + \kappa_{X_{v_r r}} X'_{v_r r} v_r' r' + \kappa_{v_r^2 r^2} X'_{v_r^2 r^2} v_r'^2 r'^2 \tag{8}$$

In the equation (5), c is the weighted average flow speed over the rudder, which is evaluated as a sum of $(1-\omega)u_r$ and $u_{A\infty}$.

$$c = \sqrt{\frac{A_P}{A_R}[(1-\omega)u_r + ku_{A\infty}]^2 + \frac{A_R - A_P}{A_R}(1-\omega)^2 u_r^2} \tag{9}$$

$u_{A\infty}$ is the induced axial velocity far behind the propeller disk, which given by

$$u_{A\infty} = -(1-w)u + \sqrt{(1-w)^2 u^2 + \frac{8}{\pi}K_T(nD)^2} \tag{10}$$

e is the effective rudder angle given by Eq. (11)

$$e = \delta\frac{v}{c} + \frac{rL}{2c} \tag{11}$$

According to the parameter identification theory, the coefficients of added mass and inertia need to be estimated in advance. Slender-body approximations (Newman, 1977), originated in the field of aerodynamics, can provide a simple but effective way. It will be applied to estimate the sway forces and yaw moments during a ship manoeuvre.

$$\begin{aligned} Y_I &= -\dot{v}\left(\tfrac{1}{2}\rho\pi d^2 L\right) - \dot{r}\left(\tfrac{1}{2}\rho\pi d^2 \textstyle\int_{L/2}^{L/2} x dx\right) \\ N_I &= -\dot{v}\left(\tfrac{1}{2}\rho\pi d^2 \textstyle\int_{L/2}^{L/2} x dx\right) - \dot{r}\left(\tfrac{1}{2}\rho\pi d^2 \textstyle\int_{L/2}^{L/2} x dx\right) \end{aligned} \tag{12}$$

With the derivative with respect to $\dot{v}$ and $\dot{r}$, the non-dimensional coefficients can be obtained.

In order to estimate the hydrodynamic coefficients of equations (4-6), adjustment coefficients are introduced, which will randomly change within the interval [0.5, 1.5] in the identification process.

$$Coef_{new} = \kappa_{\text{Coef}} * Coef_0 \tag{13}$$

where, $Coef_0$ is the base values of hydrodynamic derivative of the similar ship model, which are given in (Moreira et al. 2007; Xu and Guedes Soares, 2016a).

The non-dimensional hydrodynamic coefficients of the similar ship model and the dimensional factor are presented in table 1.

Table 1. The base values of hydrodynamic derivative

Coefficient	Value	Coefficient	Value
$(m-Y_{\dot{v}})'$	0.0352	Y_0'	1.90*e-6
$(I_Z-N_{\dot{r}})'$	0.00222	Y_{v_r}'	-0.0261
$(m-X_{\dot{u}_r})'$	0.0116	Y_δ'	0.00508
η_1'	-0.962*e-5	Y_r'	0.00365
η_2'	-0.446*e-5	Y'_{rrv_r}	-0.0450
η_3'	0.0309*e-5	Y'_{eee}	-0.00185
C_R'	0.00226	N_0'	-0.00028
$X'_{v_r^2}$	-0.006	N'_{v_r}	-0.0105
X'_{ee}	-0.00224	N'_δ	-0.00283
X'_{rr}	0.00515	N'_r	-0.00480
$(X_{v_r r}+m)'$	0.0266	N'_{rrv_r}	0.00611
X'_{rrvv}	-0.00715	N'_{eee}	0.00116

3. SYSTEM IDENTIFICATION BASED ON A GLOBAL OPTIMIZATION ALGORITHM

In this section, different loss functions were firstly defined considering the effect of noise and the empirical errors, because the *true* values of hydrodynamic coefficient of ship mode was not known. A good loss function will increase the accuracy of the identified results and help to approach the *true* values. Then a global optimization algorithm, Genetic Algorithm (GA), will be introduced and the structure of the identification program will be illustrated.

It is worth to note that the input signal must change sufficiently in order to excite the system so that the experimental data contains enough information about the dynamics of the system. According the above mathematical model, the input signals for surge, sway and yaw motion are given as:

$$\begin{aligned} \varphi_u &= [u_r'^2, n'u_r', n'^2, v_r'^2, e^2, r'^2, v_r'r', v_r'^2 r'^2] \\ \varphi_v &= [u_{A\infty}'^2, v_r', r', \delta, r'^2 v_r', e^3] \\ \varphi_r &= [u_{A\infty}'^2, v_r', r', \delta, r'^2 v_r', e^3] \end{aligned} \tag{14}$$

The matrix is obtained using measured data, it usually is positive definite.

In order to measure the difference or distance between target systems output $y_i (i = 1 \cdots N)$, and the mathematical model output $\hat{y}_i (i = 1 \cdots N)$, the loss function will need to be defined. It usually has an important effect on the precision and generalization performance of the desired mathematical model. With the assumed mathematical model, which can be obtain by a mechanical analysis or a priori considerations, the

parameter identification consists in seeking values that would minimize the loss function. Some popular loss functions can be defined:

The L^1-norm can be written as:

$$F^1(y,\hat{y}) = \|y-\hat{y}\|_{L^1} = \frac{1}{N}\sum_{i=1}^{i=N}|y_i-\hat{y}_i| \quad (15)$$

The L^2-norm can be defined as follow:

$$F^2(y,\hat{y}) = \|y-\hat{y}\|_{L^2} = \frac{1}{N}\sqrt{\sum_{i=1}^{i=N}(y_i-\hat{y}_i)^2} \quad (16)$$

The L^∞-norm can be written as:

$$F^\infty(y,\hat{y}) = \|y-\hat{y}\|_{L^\infty} = \max|y_i-\hat{y}_i| \quad (17)$$

From Eqs. (15-17), the main purpose of the proposed loss function is to minimise the distance between the reference outputs and the mathematical model outputs. A good mathematical model should reproduce the reference outputs with small bias, and also with small variance. A small variance can be obtained easily with a small number of parameters. In this paper, the mathematical model was defined with a certain number of parameters in section 2. The loss function considering the bias and variance between the reference outputs and the mathematical model outputs will provide more stable mathematical model. The loss function can be defined as:

$$F^s(y,\hat{y}) = \frac{1}{N}\left(\sqrt{\sum_{i=1}^{i=N}(y_i-\hat{y}_i)^2} + \sqrt{\sum_{i=1}^{i=N}(|y_i-\hat{y}_i|-\bar{E})^2}\right) \quad (18)$$

where $\bar{E} = \sum_{i=1}^{i=N}|y_i-\hat{y}_i|/N$ is the absolute mean value of the bias of the reference outputs and the mathematical model outputs.

In order to minimise the loss function, a global optimization algorithm (GA), was applied in the process of optimal parameters search. It is a very powerful optimization method due to its inherent property of implicit parallelism (Holland, 1992; McGookin et al. 2000; Xu and Guedes Soares, 2015). It can explore a large number of potential solutions in parallel and is less likely to get stuck at a local optimum due to its mutation mechanism. The work flow of a classic GA is presented in the Figure. 3. From this figure, the main operator to work on the parents is crossover, which is applied with a certain probability (p_c). As shown in the figure 3, the crossover operator takes valuable information from both parents and combines it to generate new potential individuals. It means that the crossover operator can exploit the potential solutions in the search space. But the crossover operator can't introduce any new information into the population at the bit level (Kristinsson and Dumont, 1992), the mutation operator should be used to insure against such a loss and as a source of new bits. The mutation operator can also generate new individuals to ensure exploration of unvisited areas so that local convergence of the population can be avoided effectively.

In order to demonstrate the performance of the obtained mathematical model, statistical metrics, R^2 , is used to quantify the fit to the data. It is defined as:

$$R^2 = 1 - \frac{\sum[y_i-\hat{y}]^2}{\sum[y_i-\bar{y}]^2} \quad (19)$$

where $\bar{y}$ is the mean value of the measured data. R^2 is the ratio of the variability in the data that is not explained by the model to the total variability in the data. Straight speaking, if R^2 equal to zero, it means that the model fails to explain the measurement variability. Otherwise, if R^2 is equal to 1, it means that all the variability of measured data can be fully explained by the model. If R^2 is negative, it means the model can explain the data worse than the mean value.

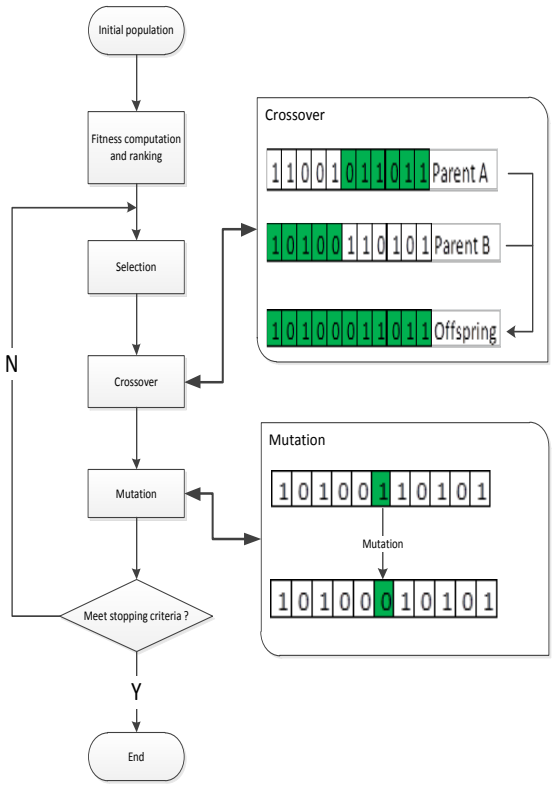

Figure 3: The work flow of a classical generic algorithm

4. FREE-RUNNING MODEL TESTS BASED ON AN AUTONOMOUS SURFACE SHIP MODEL

In this section, the results of manoeuvring tests on board an autonomous surface vehicle (ASV) are presented. The ASV is a scale model of 2.5 metres, self-propelled and equipped with navigation and positioning equipment.

The tests were conducted in a large swimming pool during the last days of March 2016.

4.1 AUTONOMOUS SURFACE SHIP MODEL PARTICULARITIES

The ASV is a scaled model of a chemical tanker that was built in Portugal, as shown in Figure 4. The model is constructed from single skin glass reinforced polyester, with plywood framings and its design speed is 0.98 m/s. Its main particulars are given in Table 2.

Figure 4: Prototype of the free-running ship model with various sensors

Table 2. Main dimensions of the model

CHEMICAL TANKER MODEL	
Length (mm)	2587.5
Breadth (mm)	426.2
Draught (estimated at the tests) (mm)	102
Propeller diameter (mm)	82.2
Design speed (m/s)	0.984
Scaling coefficient	65.7

4.2 HARDWARE STRUCTURE OF THE AUTONOMOUS SURFACE SHIP MODEL

The hardware structure consists of all sensors and actuators that are used in the ASV real-time navigation and control platform. The hardware is further divided into two units of: command and monitoring unit (CMU) and communication and control unit (CCU) (Perera et al., 2015, Hinostroza et al., 2017).

The main objective of the CMU is to facilitate manual and autonomous control of the ASV that provides a human machine interface (HMI). As presented in the Figure. 5, the CMU mainly consists of several instruments: Laptop, GPS unit, industrial wireless unit, Compact-RIO, main AC power supply unit, DC power supply unit and Anemometer.

A laptop is used in a HMI that is connected through industrial Wi-Fi unit for communication with the CCU. The laptop works as a data display unit as well as an automatic and manual control unit for the ASV. A GPS unit is used in the CMU for position measurements of the ASV. It is composed by two units of: base station and rover station. Both GPS units are used to improve the position accuracy of the ASV that is around the accuracy of ± 2 (cm). Industrial wireless unit is used for communication between the ashore based CMU and on-board CCU. The network topology in this system is considered as: ashore based CMU unit works as an "assess point" unit and on-board CCU works as a "client" unit. The shore based" assess point" unit acts as a master unit in the CMU. Furthermore, both units are configured into a bridge type Ethernet local area network (LAN), through an industrial Ethernet switch. The anemometer is used to measure the relative wind direction and wind speed at the location of tests. The compact-RIO 9074 unit consists of an industrial real-time processor with a 2M gate FPGA that has eight slots for NI C Series I/O modules with the operation power of 19 to 30 VDC. All units in the CMU are powered by the shore based main AC unit that is also complemented by a NI DC power supply unit.

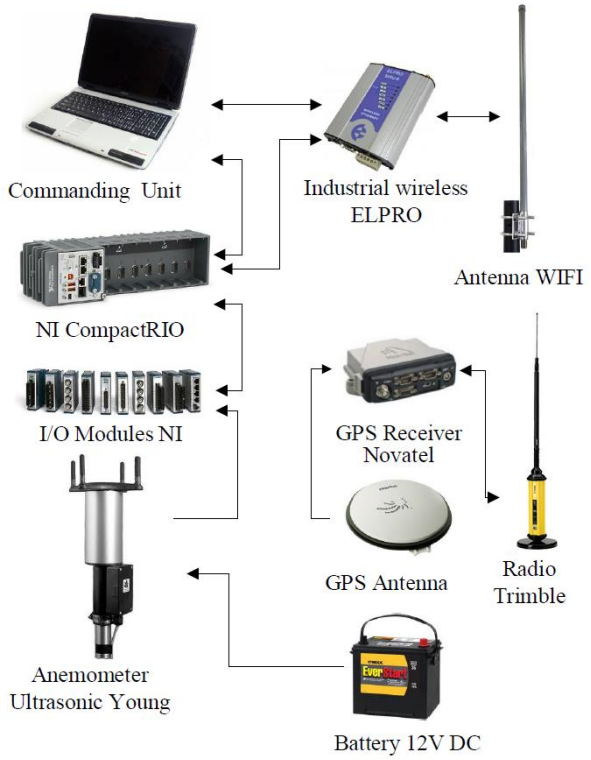

Figure 5: Command and monitoring unit at shore

The main objective of the CCU is to implement real-time control algorithms that are associated with course and speed controls of the ASV, as shown in the Figure. 6, the CCU consists of following instrumentations; Laptop, Compact-RIO, industrial Ethernet switch (IES), GPS unit, industrial wireless unit, DC motor with encoder, servo motor, fibre optic gyrocompass, batteries and fuse units.

An on-board Laptop is used as Real-time acquisition system to record, processing and display signals from the gyrocompass and GPS unit. The connection is established by RS232/USB-serial ports. A compact RIO 9004 composed by a 195 MHz industrial real-time processor with 64 MB of DRAM memory and 512 MB

of non-volatile Compact- Flash storage for data logging and that has 8 slots for NI C-series I/O modules, is used to control the propeller revolutions and rudder position. The I/O module NI 9505 full H-bridge DC servo drive is used to generate PWM and amplify current to control the motors. The Compact-RIO 9004 is powered by an on-board battery through fuse units. A HS-5685MH servomotor with high voltage, High Torque, Metal Gear is used as actuator for rudder. A DC-Maxon Brushed motor is used as actuator for the propeller. Laptop and Compact RIO units are connected through the IES for the Ethernet communication.

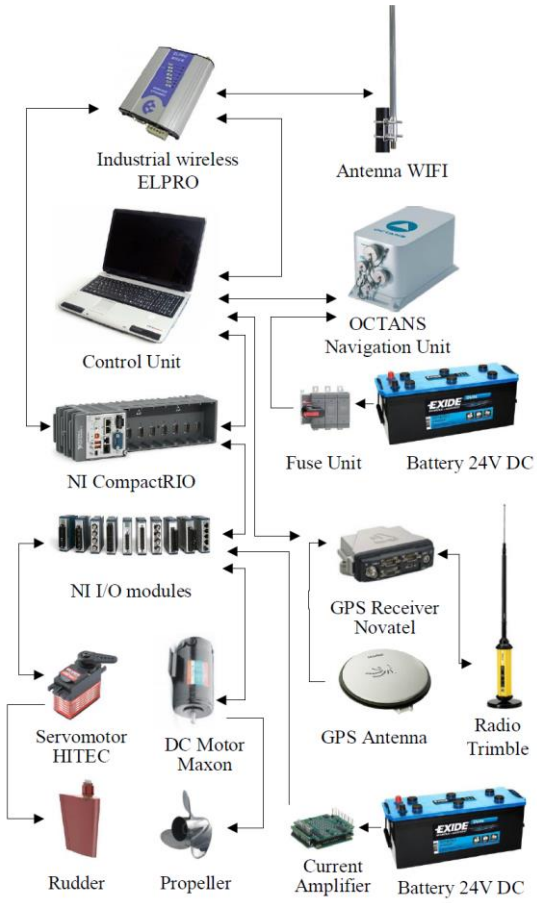

Figure 6: Equipment and sensors in communication and control unit

4.3 SOFTWARE ARCHITECTURE OF THE ASV

The software architecture is mainly programmed by LabVIEW software, as presented in Figure.7. The software architecture consists of several program loops: FPGA loop, real-time loop and TCP/IP loop. The FPGA loop is associated with collecting data from the sensors (i.e. GPS, IMS and fibre-optic gyrocompass units) and controlling the actuations of propeller and rudder sub-systems that have been programmed under a reconfigurable FPGA platform, where LabVIEW provides the VDHL software codes.

The real-time loop is associated with a reconfigurable FGPA platform and an embedded real-time processor. The associated PID controllers for rudder and propeller sub-systems are implemented under the internal deterministic control loop that has the highest responses, determinism and priority with compare to other software loops. The data processing and saving for the respective sensors are implemented under the internal non-deterministic data processing loop that has lower priority with compare to the deterministic control loop. The sensor data has been incorporated into network shared variables that are forecasted along the entire network. The TCP/IP loop is associated with a real-time processor and the HMI is used for analysis, post-processing, data logging, communications and control of the ASV. The TCP/IP loop is implemented under wireless communication through the industrial Wi-Fi unit.

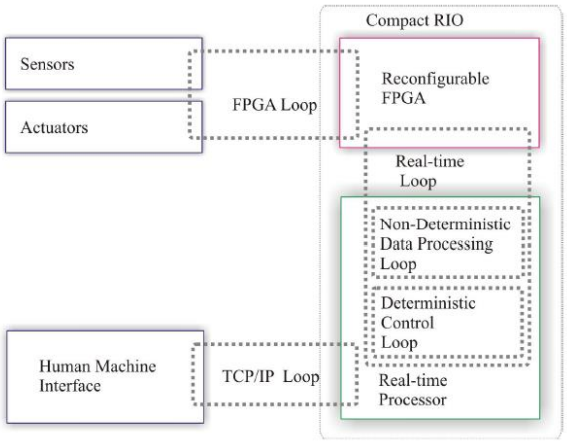

Figure 7: Software architecture

4.4 EXPERIMENTAL RESULTS OF FREE-RUNNING MODEL TESTS

Model tests on the ASV were conducted at the swimming pool of *Piscina Oceanica*, Oeiras, Portugal, seen in Figure 8. The weather was sunny and dry, but some wind was constantly present, changing its speed (approximately in the interval of 1–2 m/s) and direction as time passed. The pond was certainly deep enough to neglect any shallow-water effects. The pool has a maximum length of 50 [m] and average breadth of 20 [m].

Figure 8: Location of the free-running model tests

The RTK–GPS unit was initiated by manually fixing the coordinates of the ashore unit and then giving instructions to the on-board unit to communicate with the ground beacon station. The model was carefully launched on water and partly ballasted to get zero list and trim, although the design draught was not reached in these tests. Also, the model was not calibrated in the sense of reaching the scaled vertical position of the centre of gravity and scaled values of the moments of inertia. During all manoeuvring tests, the rpm order was kept constant.

Unfortunately, due to the restricted area available for the execution of the trajectories it was not possible to take in consideration in the contents of the trial plan all the recommendations of the trial code proposed by the Interim Standards for Ship Manoeuvrability (IMO). The manoeuvres selected to be presented in this work is the zigzag. Altogether 3 test runs were executed with ship model.

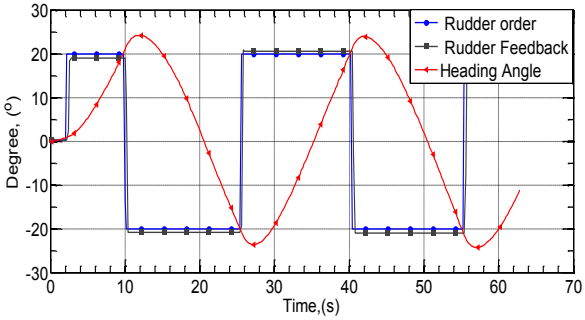

Figure 9: The $20^{\circ}-20^{\circ}$ zigzag manoeuvring test using free-running ship model

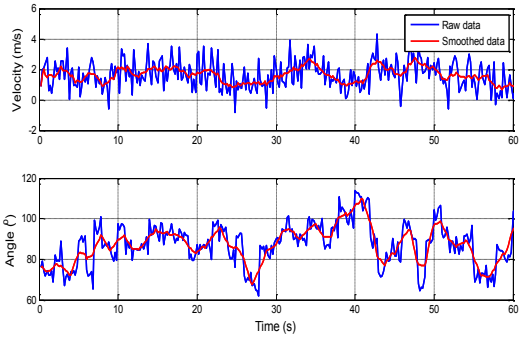

Figure 10: Wind conditions during zigzag manoeuvring tests

Figures. 9-11 present results of and Zigzag manoeuvres. The collected data have a high quality and suitable to carry out further manoeuvrability of the ship model. In the figure 10, the wind speed is about 2m/s and the direction is about . This data can be used to model the environment disturbance, especially the wind.

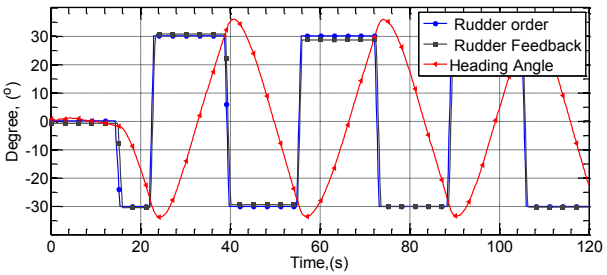

Figure 11: The $30^{\circ}-30^{\circ}$ zigzag manoeuvring test using free-running ship model

5. PARAMETER IDENTIFICATION AND VALIDATION OF THE IDENTIFICATION ALGORITHM

In this section, the nonlinear manoeuvring mathematical model with fixed structure is chosen and its parameters are identified based on the free-running model tests. The genetic algorithm discussed in the previous section will be used to minimise the loss functions. The $20^{\circ}-20^{\circ}$ zigzag manoeuvring test will be chosen as the training purpose.

As in the figure 9, the $20^{\circ}-20^{\circ}$ zigzag manoeuvring test was successfully carried out and the result is good. At the same time, the velocity of surge, sway and yaw are also recorded during the test by using the IXSEA inertial measurement unit. The results are presented in figure 12. As can be seen, the velocity of surge and sway change smoothly, but there are some oscillations of yaw rate, especially during the transition. In order to minimise the effect of noise, a moving average filter will be applied, which smooth data by replacing each data point with the average of the neighbouring data points defined within the span (Moler, 2004). This process is equivalent to low pass filtering with the response of the smoothing given by the difference equation (Eq. 18). The algorithm is also available in MATLAB (*smooth.m*). The smoothed yaw rate is also presented in the figure 8. It shows that the moving average filter works well and reduce the oscillations effectively.

$$y_s(i) = \frac{1}{2N+1}(y(i+N) + y(i+N-1) + \ldots + y(i-N)) \qquad (20)$$

Table 3. Zigzag Data recorded

Data ID	Rudder angle	Date/Hour	Data characteristics	Wind conditions
Z1	20/20 (deg.)	28042016/12:16:14	All equipment working, good data.	Moderate ≈ 2 [m/s]
Z2	25/25 (deg.)	28042016/11:15:32	Corrupted data, not presented.	Too windy ≈6 m/s
Z3	30/30 (deg.)	28042016/12:27:54	All equipment working, good data.	Moderate ≈ 2 [m/s]

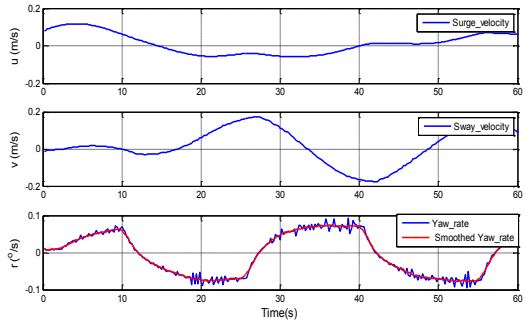

Figure 12: The velocity of surge sway and yaw from the inertial sensor during the $20^\circ - 20^\circ$ zigzag manoeuvring test.

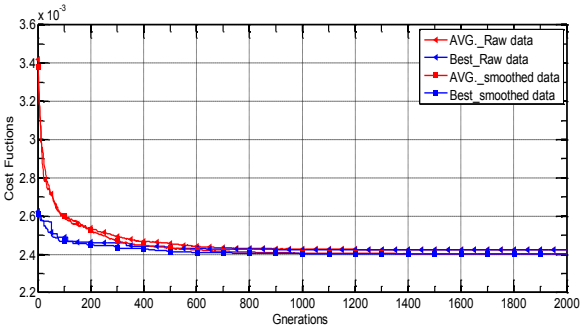

Figure 13: Evolution of the loss function values with the L^1-norm metric

Before the process of parameter identification, the parameters of generic algorithm need to be defined in advance. The size of the population was 200 individuals. The optimization process was assumed to be converged after 2000 evolutions, which was proved to be sufficient. So the total number of generations was 2000. The one-point crossover probability was 0.8 and the single-bit mutation probability was 0.02.

As mentioned in the previous section, different loss functions will be applied in the system identification process. An example of the evolution of the loss function is presented in figure 13. The evolutions can be converged whether the inputs are the raw data or the smoothed data. The only difference is that the loss function value is smaller when using the smoothed data, which also agrees with common sense. Because there are some oscillations in the raw data, which is will increase the total values of loss functions unavoidable.

The identified adjusted coefficients of the hydrodynamic parameters of nonlinear manoeuvring mathematical model are presented in table 4. Because the "true" values of the parameters of the mathematical model are never known in real-world applications, the values of the adjustment parameters should be limited in a proper range based on the similar ship model, whose hydrodynamic parameters was already known in advance. So the identification procedure will provide a mathematical model of the ship which would reasonably accurately reproduce the behaviour of the ship in manoeuvring motion. As presented in the table 4, C_R' is the resistance coefficient, which should be close to the similar ship model. It also mean that the adjusted coefficient of C_R' should be around 1. It shows that all the metrics provide good results. Some of the adjustment coefficients, namely those with subscripts Y_0' and N_0', however, kept fixed in Sutulo and Guedes Soares, (2015), because their influence is considered less important. So the adjustment coefficients should be near 1. From the table 4, the metric of L^∞ - norm provide a worse results. It is because the infinity norm does not provide sufficient information.

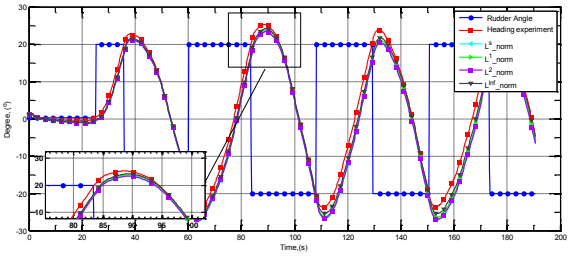

Figure 14: The $20^\circ - 20^\circ$ zigzag manoeuvring response reproduced on the basis of the parameters identified from the raw data

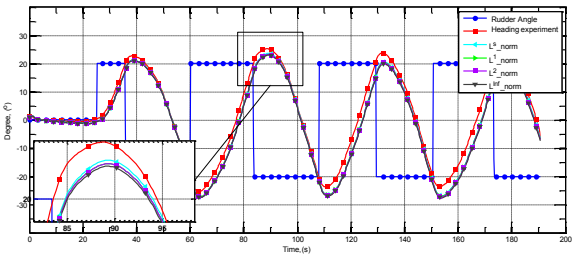

Figure 15: The $20^\circ - 20^\circ$ zigzag manoeuvring response reproduced on the basis of the parameters identified from the smoothed data

The adjustment coefficients from table 4 were later used for modifying the mathematical model and the modified model was then run to obtain verification and validation responses. The $20^\circ - 20^\circ$ and $30^\circ - 30^\circ$ zigzag manoeuvring tests, which were not used in training process, will be considered as the verifying responses although compared were time histories for the yawing angle. The comparisons of time histories obtained with identified parameters with the reference time histories for the $20^\circ - 20^\circ$ and $30^\circ - 30^\circ$ zigzag manoeuvring tests is realised in figure 14 - 17.

Table 4. The adjusted coefficients of the hydrodynamic parameters of nonlinear manoeuvring mathematical model

Subscript	L^s-norm	L^1-norm	L^2-norm	L^∞-norm	L^s-norm	L^1-norm	L^2-norm	L^∞-norm
	Raw data				Smoothed data			
η_1'	0.8189	0.7851	0.9036	0.8555	0.9314	0.9224	0.8848	0.8493
η_2'	1.0875	1.0899	0.9439	0.9286	1.0245	1.0240	0.9382	1.1379
η_3'	0.5050	0.5058	0.5073	0.5239	0.5125	0.5049	0.5130	1.1677
C_R'	1.0197	0.9724	0.9968	1.0811	1.0868	0.9434	0.9982	0.9978
$X'_{v_r^2}$	0.5048	0.5112	0.5052	0.5606	0.5035	0.5075	0.5032	0.5274
X'_{eee}	0.5825	0.5235	0.5477	0.9796	0.5662	0.6053	0.5640	0.9464
X'_{rr}	1.3853	1.3080	1.3335	1.3363	1.3400	1.3126	1.2933	0.8551
$X'_{v_r r}+m'$	0.5008	0.5003	0.5008	0.5025	0.5004	0.5003	0.5008	0.5015
X'_{rrvv}	0.5022	0.5040	0.5028	0.5366	0.5031	0.5050	0.5013	0.5038
Y_0'	0.8950	1.0583	0.9609	0.9513	0.9246	0.9508	0.9280	0.8879
Y_{v_r}'	0.5036	0.5132	0.5066	0.5280	0.5060	0.5102	0.5100	0.5089
Y_δ'	0.5081	0.5118	0.5092	0.5122	0.5081	0.5055	0.5018	0.5073
Y_r'	0.5178	0.5170	0.5256	0.5262	0.5217	0.5053	0.5157	0.5250
Y'_{rrv_r}	0.5006	0.5022	0.5019	0.5009	0.5011	0.5027	0.5036	0.5011
Y'_{eee}	1.1391	1.0310	1.1637	1.1185	1.0277	1.2124	0.9931	1.0040
N_0'	1.0302	1.0507	0.9962	0.5666	0.9231	1.0123	1.0418	1.1430
N'_{v_r}	1.3377	1.3455	1.2113	1.1521	1.3984	1.1732	1.2636	1.2491
N'_δ	0.5307	0.5171	0.5431	0.5352	0.5117	0.5137	0.5115	0.5357
N_r'	0.5170	0.5127	0.5097	0.5265	0.5203	0.5168	0.5102	0.5393
N'_{rrv_r}	0.5060	0.5300	0.5143	0.5094	0.5065	0.5168	0.5080	0.5125
N'_{eee}	0.8515	0.9980	1.0670	1.0187	1.1017	1.0600	1.0524	0.8764

The identified parameters, which were obtained using the previous mentioned loss functions with the raw data, were used to compare the zigzag $20^\circ - 20^\circ$ manoeuvring test firstly. In figure 14, the heading angle output was reproduced very well on the basis of the parameters identified from the raw data when all metrics were used. It has to be mentioned that L^∞-norm metric also demonstrated good results, although it can't provide reasonable parameters. When the identified parameters obtained from smoothed data were used, the heading responses were presented in figure 15. In this figure, L^s-norm metric demonstrated better reproducibility in all smoothed cases. It means that the filter technology for inputs is very necessary when implying the system identification. From the figure 14-17, the metrics L^s-norm and L^1-norm demonstrated a good result.

In order to verify the generalization of the performance of the proposed parameter identification technology, a large rudder deflection test, the $20^\circ - 20^\circ$ zigzag manoeuvring test was also carried out, and the result will be compared with the yawing angle response of the identified nonlinear mathematical models. The results are presented in figures 16-17. The response history of yawing angle of the nonlinear manoeuvring mathematical model on the basis of the parameters identified from the raw data is presented in figure 16. As shown in the figures, the models can provide an accurate response compared with the experiment values. It also demonstrated that the identified mathematical model can be used for a large rudder deflection manoeuvring test. The goodness of fit criterion, R^2, is given in Table 5-6. The obtained parameters can provide a good prediction of zigzag manoeuvring response.

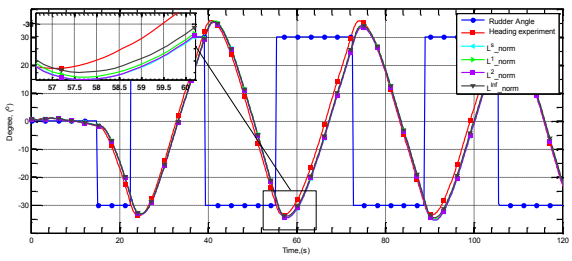

Figure 16: The $30^\circ - 30^\circ$ zigzag manoeuvring response reproduced on the basis of the parameters identified from the raw data

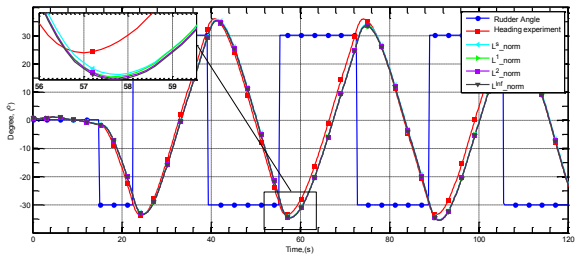

Figure 17 The $30^\circ - 30^\circ$ zigzag manoeuvring response reproduced on the basis of the parameters identified from the smoothed data

Table 5. The R^2 goodness of fit criterion of $20^\circ - 20^\circ$ zigzag manoeuvring test

	L^s-norm	L^1-norm	L^2-norm	L^∞-norm
Raw data	0.9613	0.9720	0.9628	0.9532
Smoothed data	0.9650	0.9623	0.9595	0.9435

Table 6. The R^2 goodness of fit criterion of $30^\circ - 30^\circ$ zigzag manoeuvring test

	L^s-norm	L^1-norm	L^2-norm	L^∞-norm
Raw data	0.9838	0.9854	0.9841	0.9776
Smoothed data	0.9842	0.9842	0.9837	0.9728

6. CONCLUSION

In this paper, system identification based on free-running tests has been used to estimate the hydrodynamic coefficients of autonomous surface ship model. A guidance, control and navigation system have been programed in the LabVIEW platform and implemented on a scaled chemical tanker ship model. Manoeuvring tests proposed by the Interim Standards for Ship Manoeuvrability (IMO) were carried out and the results were used for training and validation purpose. In order to make the modelling more flexible and physically more realistic, the classical nonlinear Abkowitz model has been modified by including the rotation speed of the propeller and the flow velocity over rudder. The flow velocity over rudder was used to nondimensionalize the forces and moment induced by rudder deflection, due to the complicated fluid region around the rudder. An offline parameter identification algorithm has been programmed, and different loss functions have been defined for minimising the distance between target systems output and the mathematical model output. The evaluation of the stability and generalization was also included in the loss function. A global optimization algorithm has been implied to minimise the loss functions and search the optimum parameters. In order to reduce the effect of noise, a low pass filtering technology has been applied to smooth the data. The adjusted coefficients of the hydrodynamic parameters of nonlinear manoeuvring mathematical model were obtained using the different metrics, and then used for reproducing the zigzag manoeuvring response.

The $20^\circ - 20^\circ$ and $30^\circ - 30^\circ$ zigzag manoeuvring tests, which were not used for training purposes, were used for validation. By comparing the predicted response with experiment, the metric of L^∞ - norm cannot provide reasonable parameters, it is because the infinity norm does not provide sufficient information. The metrics L^s-norm and L^1-norm usually demonstrated a good result, and have a good agreement with the experiment. The system identification technology proposed in this paper is quite encouraging for manoeuvring modelling of surface ship base on free-running model tests. The comparison with experiment also demonstrated the validity of the proposed identification technology.

7. ACKNOWLEDGEMENTS

This work was performed within the Strategic Research Plan of the Centre for Marine Technology and Ocean Engineering (CENTEC), which is financed by Portuguese Foundation for Science and Technology (Fundação para a Ciência e Tecnologia-FCT). The experiments with the vessel model were not possible without the collaboration of Eng. José Costa, Coordinator of the "Piscina Oceanica", Oeiras, Portugal, who allowed the realization of the maneuvering tests in their installations. The authors are grateful to FP Santos for his help during the execution of the model tests.

8. REFERENCES

1. ABKOWITZ, M. A. *Measurement of hydrodynamic characteristics from ship maneuvring trials by system identification*. SNAME Transactions, 88, 283–318. (1980)
2. AKANYETI, O., NEHMZOW, U., & BILLINGS, S. A. *Robot training using system identification*. Robotics and Autonomous Systems, 56(12), 1027-1041. (2008)
3. ALONGE, F., D'IPPOLITO, F., & RAIMONDI, F. M. *Least squares and genetic algorithms for parameter identification of induction motors*. Control Engineering Practice, 9(6), 647-657. (2001)
4. ÅSTRÖM, K. J., and KÄLLSTRÖM, C. G. *Identification of ship steering dynamics*. Automatica, 12(1), 9–22. (1976)
5. CASENAVE, C., MONTSENY, E., AND CAMON, H. *Identification of nonlinear dynamic models of electrostatically actuated MEMS*. Control Engineering Practice, 18(8), 954-969. (2010)

6. CHEN, T., and LJUNG, L. *Implementation of algorithms for tuning parameters in regularized least squares problems in system identification*. Automatica, 49 (7), pp: 2213-2220. (2013)
7. DAI, S.-L., WANG, C., and LUO, F. *Identification and Learning Control of Ocean Surface Ship Using Neural Networks*. IEEE Transactions on Industrial Informatics, 8(4), 801–810. (2012)
8. ELOOT, K., and VANTORRE, M. *Alternative captive manoeuvring tests: possibilities and limitations*. In Symposium on forces acting on a manoeuvring vessel (MAN98) (pp. 16–18). Val de Reuil, France. (1998)
9. FALCK, T., DREESEN, P., DE BRABANTER, K., PELCKMANS, K., DE MOOR, B., & SUYKENS, J. A. (2012). *Least-squares support vector machines for the identification of Wiener–Hammerstein systems*. Control Engineering Practice, 20(11), 1165-1174.
10. HINOSTROZA M.A., XU HAITONG & GUEDES SOARES C. (2017), *Path-planning and path-following control system for autonomous surface vessel, Maritime Transportation and Harvesting of Sea Resources*, Taylor & Francis Group, London, pp.991-998.
11. HOLLAND, J. *Adaptation in natural and artificial systems : an introductory analysis with applications to biology, control, and artificial intelligence*. MIT Press. (1992)
12. ITTC. *The Manoeuvring Committee - Final Report and Recommendations*. Proceedings of 23rd ITTC. Venice. (2002)
13. IGLESIAS, R., NEHMZOW, U., & BILLINGS, S. A. *Model identification and model analysis in robot training*. Robotics and Autonomous Systems, 56(12), 1061-1067. (2008)
14. KÄLLSTRÖM, C. G., AND ÅSTRÖM, K. J. *Experiences of system identification applied to ship steering*. Automatica, 17(1), 187–198. (1981)
15. KON, J., YAMASHITA, Y., TANAKA, T., TASHIRO, A., and DAIGUJI, M. *Practical application of model identification based on ARX models with transfer functions*. Control Engineering Practice, 21(2), 195-203. (2013)
16. KRISTINSSON, K., and DUMONT, G. A. *System identification and control using genetic algorithms*. IEEE Transactions on Systems, Man, and Cybernetics, 22(5), 1033–1046. (1992)
17. KYRIACOU, T., NEHMZOW, U., IGLESIAS, R. and BILLINGS, S. A. *Accurate robot simulation through system identification*. Robotics and Autonomous Systems, 56(12), 1082-1093. (2008)
18. LJUNG, L. *System Identification: Theory for User*. Prentice-Hall (Vol. 11). Englewood Cliffs, N.J. (1987)
19. LUO, W., GUEDES SOARES, C., and ZOU, Z. *Parameter Identification of Ship Maneuvering Model Based on Support Vector Machines and Particle Swarm Optimization*. Journal of Offshore Mechanics and Arctic Engineering, 138(3), 31101. (2016)
20. LUO, W., MOREIRA, L., and GUEDES SOARES, C. *Manoeuvring simulation of catamaran by using implicit models based on support vector machines*. Ocean Engineering, 82, 150–159. (2014)
21. MCGOOKIN, E. W., MURRAY-SMITH, D. J., LI, Y., and FOSSEN, T. I. *Ship steering control system optimisation using genetic algorithms*. Control Engineering Practice, 8(4), 429–443. (2000)
22. MOLER, C. *Numerical Computing with MATLAB*. Philadelphia: SIAM. (2004)
23. MOREIRA, L., FOSSEN, T. I., and GUEDES SOARES, C. *Path following control system for a tanker ship model*. Ocean Engineering, 34(14), 2074–2085. (2007)
24. MOREIRA, L., and GUEDES SOARES, C. *Dynamic model of manoeuvrability using recursive neural networks*. Ocean Engineering, 30(13), 1669–1697. (2003)
25. MOREIRA, L., and GUEDES SOARES, C. *Recursive neural network model of catamaran manoeuvring*. Transactions of the Royal Institution of Naval Architects Part A: International Journal of Maritime Engineering, 154 (Part A3), 121–130. (2012)
26. MOREIRA, L., and GUEDES SOARES, C. *Autonomous Ship Model to Perform Manoeuvring Tests*. Journal of Maritime Research, 8(2), 29–46. (2014)
27. MORENO-SALINAS, D., CHAOS, D., DE LA CRUZ, J. M., ARANDA, J., ARANDA, J. *Identification of a Surface Marine Vessel Using LS-SVM*. Journal of Applied Mathematics, 2013, 1–11. (2013)
28. NEWMAN, J. N. *Marine hydrodynamics*. Massachusetts, USA: MIT Press. (1977)
29. PERERA, L., MOREIRA, L., SANTOS, F. S. SUTULO, and C. GUEDES SOARES. *A navigation and control platform for real-time manoeuvring of autonomous ship models*. In Proc. 9th IFAC Conference on Manoeuvring and Control of Marine Craft (MCMC 2012) (pp. 465–470). Arenzano, Italy. (2012)
30. PERERA, L. P., FERRARI, V., SANTOS, F. P., HINOSTROZA, M. A., and GUEDES SOARES, C. *Experimental Evaluations on Ship Autonomous Navigation and Collision Avoidance by Intelligent Guidance*. IEEE Journal of Oceanic Engineering, 40(2), 374–387. (2015a)
31. PERERA, L. P., OLIVEIRA, P., and GUEDES SOARES, C. *System Identification of Nonlinear*

Vessel Steering. Journal of Offshore Mechanics and Arctic Engineering, 137(3), 31302. (2015b)

32. PERERA, L. P., OLIVEIRA, P., and GUEDES SOARES, C. *System Identification of Vessel Steering With Unstructured Uncertainties by Persistent Excitation Maneuvers*. IEEE Journal of Oceanic Engineering, 1–14. (2016)
33. RAJESH, G., RAJASEKHAR, G. G., and BHATTACHARYYA, S. K. *System Identification for Nonlinear Maneuvering of Ships Using Neural Network*. Journal of Ship Research, 54.1, 1–14.
34. REVESTIDO HERRERO, E., and VELASCO GONZÁLEZ, F. J. (2012). *Two-step identification of non-linear manoeuvring models of marine vessels*. Ocean Engineering, 53, 72–82. (2010)
35. SCHAFROTH, D., BERMES, C., BOUABDALLAH, S., and SIEGWART, R. *Modeling, system identification and robust control of a coaxial micro helicopter*. Control Engineering Practice, 18(7), 700-711. (2010)
36. SÖDERSTRÖM, T. *Errors-in-variables methods in system identification*. Automatica, 43(6), 939–958. (2007)
37. SÖDERSTRÖM, T. *System identification for the errors-in-variables problem*. In UKACC International Conference on CONTROL 2010 (pp. 19–32). Institution of Engineering and Technology. (2010)
38. SÖDERSTRÖM, T. *Comparing some classes of bias-compensating least squares methods*. Automatica, 49(3), pp.840-845. (2013)
39. SÖDERSTRÖM, T., MAHATA, K., and SOVERINI, U. *Identification of dynamic errors-in-variables models: Approaches based on two-dimensional ARMA modeling of the data*. Automatica , 39(5), pp.929-935. (2003)
40. SÖDERSTRÖM, T., and STOICA, P. G. *System identification*. Prentice Hall. (1989)
41. SUTULO, S., and GUEDES SOARES, C. *An algorithm for offline identification of ship manoeuvring mathematical models from free-running tests*. Ocean Engineering, 79, 10–25. (2014)
42. SUTULO, S., and GUEDES SOARES, C. *Offline system identification of ship manoeuvring mathematical models with a global optimization algorithm*. In MARSIM 2015 (pp. 8–11). Newcastle University, United Kingdom. (2015)
43. TAFNER, R., REICHHARTINGER, M. and HORN, M., *Robust online roll dynamics identification of a vehicle using sliding mode concepts*. Control Engineering Practice, 29, pp.235-246.(2014)
44. TANG, S., ZHENG, Z., QIAN, S. and ZHAO, X., *Nonlinear system identification of a small-scale unmanned helicopter*. Control Engineering Practice, 25, pp.1-15. (2014)
45. XU, H., & GUEDES SOARES, C. *An optimized path following algorithm for a surface ship model*. Guedes Soares, C., Dejhalla, R. and Pavletiæ, D. (Eds), Towards Green Marine Technology and Transport, Taylor & Francis Group 151–158. (2015)
46. XU, H., and GUEDES SOARES, C. *Vector field path following for surface marine vessel and parameter identification based on LS-SVM*. Ocean Engineering, 113, 151–161. (2016a)
47. XU, H., and GUEDES SOARES, C. *Waypoint-following for a marine surface ship model based on vector field guidance law*. In (Eds.) Guedes Soares, C. and Santos T. A. (Ed.), Maritime Technology and Engineering 3 London, UK: Taylor & Francis Group. pp. 409–418). (2016b)
48. YOON, H. K., and RHEE, K. P. *Identification of hydrodynamic coefficients in ship maneuvering equations of motion by Estimation-Before-Modeling technique*. Ocean Engineering, 30(18), 2379–2404. (2003)
49. ZHANG, X. G., and ZOU, Z. J. *Identification of Abkowitz model for ship manoeuvring motion using ε-support vector regression*. Journal of Hydrodynamics, 23(3), 353–360. (2011)

